

Self-consistent diffusion approach to CO₂ vibrational kinetics

P. Viegas¹, M. C. M. van de Sanden¹, S. Longo² and P. Diomedè¹

¹Center for Computational Energy Research, DIFFER - Dutch Institute for Fundamental Energy Research, De Zaale 20, 5612 AJ Eindhoven, the Netherlands

²Dipartimento di Chimica, Università degli Studi di Bari, via Orabona 4, 70126 Bari, Italy

Abstract: The vibrational kinetics of the CO₂ asymmetric stretching mode is analysed numerically through two different methods: a full State-To-State (STS) model and a simplified STS model for the first vibrational levels consistently coupled to the solution of the Fokker-Planck (FP) equation in the vibrational energy space. Results obtained with the two methods are compared and it is shown that consistent results can be obtained with higher computational efficiency using the FP approach.

Keywords: CO₂ dissociation, vibrational kinetics, Fokker-Planck equation

1. Introduction

In recent years, much attention has been dedicated to low-temperature plasmas to convert greenhouse CO₂ into new carbon-neutral fuels or useful chemicals [1]. Vibrational excitation of the CO₂ molecule plays an important role in energy-efficient non-equilibrium dissociation kinetics. The main tool used to study vibrational kinetics is the state-to-state (STS) finite rate method, based on the numerical solution of a master equation (ME). This last is actually a stiff system of nonlinear Ordinary Differential Equations (ODEs), as many as the number of vibrational levels. When polyatomic molecules are involved, with a high number of vibrational levels and transitions, the computational efficiency of models describing reactors with spatial resolution and coupling different physical phenomena is compromised. Such models require new methods allowing a significant reduction in computational cost.

In our previous publications [2, 3], we have proposed, as an alternative, a numerical method based on the diffusion formalism developed in the past for analytical studies [4]. The vibrational distribution function (VDF) representing the populations of the asymmetric stretching mode of CO₂ on a continuous internal energy scale has been calculated through the resolution of the drift-diffusion Fokker-Planck (FP) equation with fixed input vibrational temperature (T_v). The numerical solution has been accomplished through the time-dependent diffusion Monte Carlo method in [2] and in stationary condition by the flux-matching approach in [3]. In this work, the FP equation is solved for T_v self-consistently calculated from a simplified STS model. Results are compared to the ones obtained through a full STS model.

2. Computational methods

a. Full State-To-State (STS) approach

The temporal evolution of the number densities of each species i is calculated by the solution of the rate equations:

$$\frac{dn_i}{dt} = \sum_j S_{ij}(t) \quad (1)$$

where n_i is the number density of species i and S_{ij} is the source/loss term associated to reaction j . A total of 24 species is considered in a pure CO₂ plasma: all the states of the vibrational asymmetric stretching mode of CO₂ (CO₂($v=n$), with n the vibrational quantum number from 0 to 21), together with electrons and the positive ion CO₂⁺. The vibrational kinetics is described by a total of 253 reactions, listed in Table 1, and with rate coefficients from [5]. In Table 1, eV indicates vibrational excitation/de-excitation by electron impact, VV vibrational-vibrational energy exchange, VT vibrational-translational energy exchange.

Table 1. List of processes in the full STS model.

Process name	Reaction
Ionization	$e + \text{CO}_2(v=0) \rightarrow \text{CO}_2^+ + 2e$
Recombination	$e + \text{CO}_2^+ \rightarrow \text{CO}_2(v=0) (\text{CO} + \text{O}, \text{C} + \text{O}_2)$
eV	$e + \text{CO}_2(v=0) \leftrightarrow \text{CO}_2(v=1-21) + e$
VV	$\text{CO}_2(v=n) + \text{CO}_2(v=1) \leftrightarrow \text{CO}_2(v=n+1) + \text{CO}_2(v=0)$ $\text{CO}_2(v=n) + \text{CO}_2(v=n) \leftrightarrow \text{CO}_2(v=n+1) + \text{CO}_2(v=n-1)$
VT	$\text{CO}_2(v=n) + \text{CO}_2 \leftrightarrow \text{CO}_2(v=n-1) + \text{CO}_2$
Dissociation	$\text{CO}_2(v=21) + \text{CO}_2(v=1) \rightarrow (\text{CO} + \text{O}) + \text{CO}_2(v=0)$ $\text{CO}_2(v=21) + \text{CO}_2(v=21) \rightarrow (\text{CO} + \text{O}) + \text{CO}_2(v=20)$

We consider a pressure $p = 2660$ Pa, fixed gas temperature $T_g = 300$ K and gas density $N = 6.43 \times 10^{17}$ cm⁻³. We assume a constant power density P_{dep} transferred to the electrons and thus the temporal evolution of the electron mean energy ϵ is described by the electron energy equation

$$\frac{d(n_e \epsilon)}{dt} = P_{dep}(t) - \frac{P_{el}}{N}(\epsilon) \times N \times n_e - \frac{P_{inel}}{N}(\epsilon) \times N \times n_e \quad (2)$$

where n_e is the electron number density and P_{el} and P_{inel} are the components of the power lost by electrons through elastic and inelastic collisions, respectively. The electron-impact rate coefficients and the electron power losses are obtained as function of ϵ from the Electron Energy Distribution Function (EEDF) solution from the Electron Boltzmann Equation (EBE) solver BOLSIG+ [6], using the

electron-impact cross sections from the Phelps database in LXcat [7]. The set of ODEs is solved until reaching a stationary condition with the solver RADAU5, an implicit Runge-Kutta method of order 5 [8]. We take as initial conditions $n_e = [\text{CO}_2^+] = 4.0 \times 10^{10} \text{ cm}^{-3}$ and $\varepsilon = 1.0 \text{ eV}$. An example of temporal evolutions of species number densities obtained with this model is presented in Fig. 1, using as input power density $P_{dep} = 100 \text{ Wcm}^{-3}$.

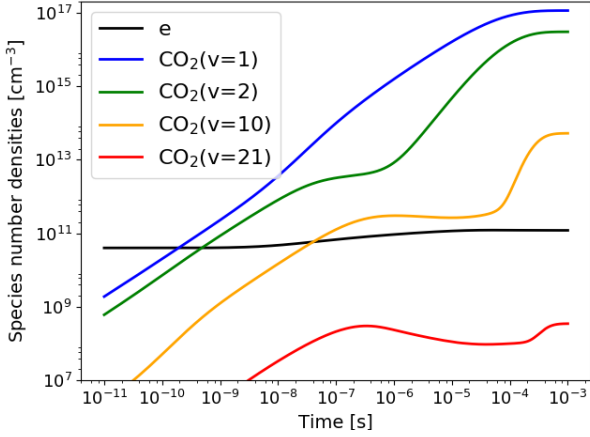


Fig. 1. Temporal evolution of species number densities using the full STS model with $P_{dep} = 100 \text{ Wcm}^{-3}$.

b. Fokker-Planck (FP) approach

The FP equation allows one to describe the evolution of the VDF f as a transport process in the space of energy ε_v of the vibrational asymmetric stretching mode, as follows:

$$\frac{df}{dt} = \frac{dJ}{d\varepsilon_v}; J = a f - b \frac{df}{d\varepsilon_v} \quad (3)$$

where $J(\varepsilon, t)$ is the flux in energy space and a and b are, respectively, the drift and diffusion coefficients, functions of T_g , T_v and the VV and VT rate coefficients, as described in [3]. In this work, T_g is fixed and the rate coefficients are the same as those used in the STS model presented in the previous section. The new approach we present in this work consists in solving a simplified STS model that allows to calculate the temporal evolution of the vibrational temperature T_v until reaching a stationary condition, coupled to the resolution of the FP equation for $df/dt = 0$ through the flux-matching method presented in [3]. The flux J (which is a constant under stationary conditions) is determined by the VV dissociation processes of Table 1 with rate coefficients $k_d^{1,21}$ and $k_d^{21,21}$:

$$J = f(\varepsilon_{max}) \frac{1}{N} (k_d^{1,21} n_1 + k_d^{21,21} f(\varepsilon_{max})) \quad (4)$$

where $\varepsilon_{max} = 5.467 \text{ eV}$, $f(\varepsilon_{max})$ is the number density at the dissociation energy and n_1 is the number density of level $v = 1$.

The simplified STS model contains the same ionization and recombination processes as the full STS model (Table 1), as well as the eV, VV and VT processes for the

vibrational levels $v \leq 2$. Hence, it contains 5 species and 15 reactions, much less than in the full STS model. T_v is calculated in both full and reduced STS models assuming a Boltzmann distribution as:

$$T_v = - \frac{E_1}{k_B \log(n_1/n_0)} \quad (5)$$

where E_1 is the energy of the vibrational level $v = 1$ and n_1 and n_0 are the number densities of levels $v = 1$ and $v = 0$ respectively.

3. Model comparison

a. Base case

For the particular case with transferred power density $P_{dep} = 100 \text{ Wcm}^{-3}$, the full STS calculation has reached a stationary condition at $t = 1.003 \text{ ms}$ with electron density and temperature $n_e = 1.2 \times 10^{11} \text{ cm}^{-3}$ and $T_e = 0.83 \text{ eV}$. With the model using a simplified STS calculation, the stationary condition has been reached at $t = 1.320 \text{ ms}$ with the same n_e and T_e . Concerning vibrational kinetics, the results using the full and simplified STS calculations are only slightly different. Fig. 2 shows the temporal evolution of T_v calculated through Eq. (5) with both models.

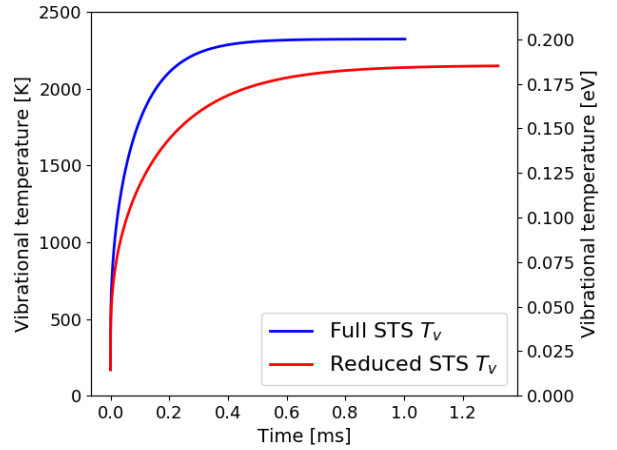


Fig. 2. Temporal evolution of T_v using both full and reduced STS models with $P_{dep} = 100 \text{ Wcm}^{-3}$.

The temporal evolution of T_v has the same trend with both models. When the stationary condition is reached, T_v is 2335 K in the full STS model and 2148 K in the reduced STS model. The difference may be due to truncating the vibrational kinetics scheme at $v = 2$ in the reduced STS calculation. Once the stationary condition is reached, the FP equation is solved for $T_v = 2148 \text{ K}$. The resulting VDF is presented in Fig. 3 and compared to the VDF obtained with the full STS model in stationary condition.

Fig. 3 shows that the VDFs obtained by the two methods are close, even though there are visible discrepancies in the VDF tail. Moreover, the dissociation rate due to the VV processes listed in Table 1 is calculated in the full STS model as $4.76 \times 10^{13} \text{ cm}^{-3}\text{s}^{-1}$. Using the FP approach, the rate of dissociation through the same processes is

calculated from Eq. 4 as $J \times N$ and is less than an order of magnitude higher: $2.28 \times 10^{14} \text{ cm}^{-3}\text{s}^{-1}$. This difference is a result of the discrepancies in the VDF tail. In a more complete model, the dissociation rate is then used to calculate the densities of other species and ultimately to calculate the conversion degree in the plasma. This result shows that an accurate trend can be obtained using the FP approach self-consistently coupled with a reduced STS model.

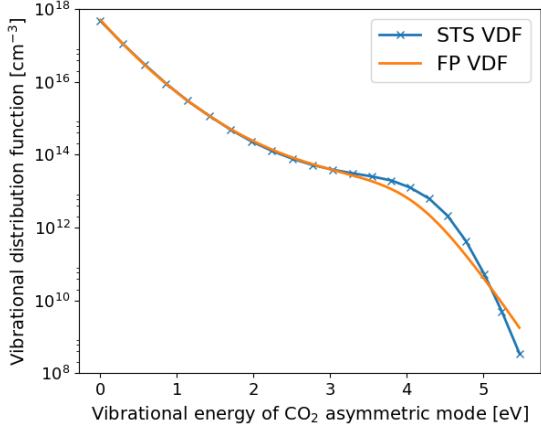


Fig. 3. Vibrational distribution function in stationary condition, using the full STS model (blue curve with crosses) and the FP equation (orange curve).

It is worth noticing that with the full STS model, the calculation time until reaching the stationary condition is of 377.7 s (~ 6 min). Although acceptable in zero-dimensions, we should notice that in multidimensional fluid models this calculation time would be multiplied by thousands or millions, and thus the total calculation time could compromise the computational cost of such models. On the other hand, with the model coupling a simplified STS calculation with the FP equation, the stationary condition is reached with a calculation time of only 52.9 s (52.8 s for the simplified STS calculation + 0.1 s for the resolution of the FP equation), seven times lower than the full STS calculation. The difference is fundamentally due to the fast semi-analytical solution which is possible for the FP equation and shows the computational gain that can be obtained through the FP approach.

b. Variation of input power density

By changing the input parameter P_{dep} , we can assess the validity of the FP approach for different conditions by comparing the results with the two models. In Table 2 are listed the resulting T_v obtained with the full and reduced STS calculations in stationary condition for transferred power densities P_{dep} between 40 and 140 Wcm^{-3} .

Table 2. Vibrational temperatures obtained in stationary condition with the full and reduced STS schemes for different P_{dep} .

P_{dep} [Wcm^{-3}]	Full STS T_v [K]	Reduced STS T_v [K]
40	1781	1523
60	2024	1762
80	2204	1967
100	2335	2148
120	2429	2312
140	2500	2463

As expected, with higher P_{dep} there is more electron production and vibrational excitation, thus increasing T_v . T_v obtained with the reduced STS calculation is consistently lower than the one calculated with the full STS scheme, the difference being below 300 K.

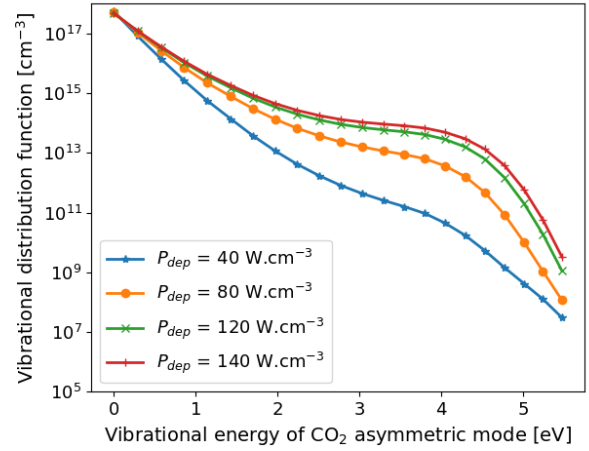


Fig. 4. Vibrational distribution functions in stationary condition, using the full STS approach for different P_{dep} .

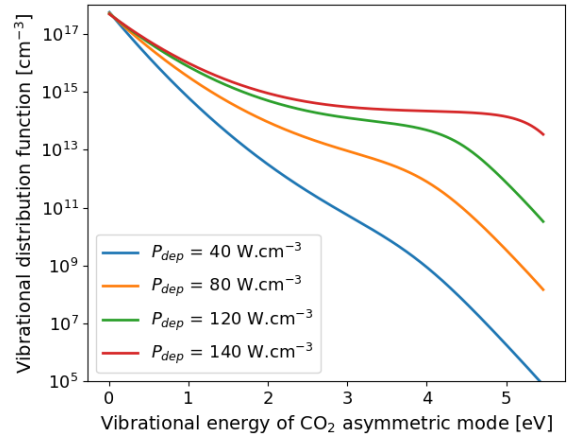


Fig. 5. Vibrational distribution functions in stationary condition, using the FP approach for different P_{dep} .

The effect of P_{dep} variation on the VDF obtained through the full STS approach is shown in Fig. 4 and the one calculated through the FP approach can be observed in Fig. 5.

We can notice that relatively small variations of T_v can significantly change the VDF. In particular, using the FP approach, $f(\epsilon_{max})$ increases around 9 orders of magnitude from $P_{dep} = 40 \text{ Wcm}^{-3}$ until $P_{dep} = 140 \text{ Wcm}^{-3}$. With the STS approach, the variation of density of level $v = 21$ is of only 3 orders of magnitude. The FP method produces VDFs overall very similar to the STS ones, also reproducing the features, variations and trends while changing the power. The changes on the VDF obviously impact the VV dissociation rate. This influence can be observed in Table 3 as function of P_{dep} .

Table 3. Dissociation rates in stationary condition with the full STS and FP approaches for different P_{dep} .

$P_{dep} [\text{Wcm}^{-3}]$	Diss. rate STS [$\text{cm}^{-3}\text{s}^{-1}$]	Diss. rate FP [$\text{cm}^{-3}\text{s}^{-1}$]
40	2.99×10^{12}	5.67×10^9
60	6.60×10^{12}	6.51×10^{11}
80	1.52×10^{13}	1.68×10^{13}
100	4.76×10^{13}	2.28×10^{14}
120	1.59×10^{14}	4.61×10^{15}
140	4.78×10^{14}	1.25×10^{19}

The dissociation rates in Table 3 reflect the dependence of the VDF on P_{dep} observed in Figs. 4 and 5. We should notice that, while the difference between the dissociation rates calculated with the two models remains lower than one order of magnitude between $P_{dep} = 60 \text{ Wcm}^{-3}$ and $P_{dep} = 100 \text{ Wcm}^{-3}$, it becomes clearly excessive for the lowest and highest values of P_{dep} considered here. Progresses in the determination of the transport coefficients from chemical rate coefficients should reduce these differences while keeping the clear advantage in terms of computational cost.

4. Conclusions

The vibrational kinetics of the CO_2 asymmetric stretching mode has been studied numerically in conditions of fixed gas temperature and transferred power density in a pure CO_2 plasma. The solution has been obtained with the classical STS approach and with a new approach introduced here: the resolution of a simplified STS model coupled to the calculation of the VDF in stationary conditions by solving the FP equation in the vibrational energy space. The results obtained through the two methods have been compared and it has been shown that T_v can be reasonably estimated from a reduced STS scheme with only vibrational levels $v \leq 2$. Hence, the FP approach can be used in self-consistent plasma models. The accuracy of the FP approach, *i.e.* the agreement between the FP and STS approaches on the resulting VDFs and dissociation rates, has been shown to be dependent on the choice of the input deposited power density and thus on T_v . The difference in the resulting dissociation rates is lower than one order of magnitude for P_{dep} between 60 Wcm^{-3} and 100 Wcm^{-3} . In the cases under study, the use of the FP approach is about seven times more computationally efficient than the full STS approach. The result on computational efficiency is very promising for the development of more

complete multidimensional fluid models to describe discharge reactors.

In the near future, we plan to correct the discrepancies in the VDF between the two approaches. The present set of transport coefficients used in the FP equation is preliminary and can be significantly improved. Moreover, we will include more complete chemistry in the CO_2 plasma model and couple it with the EEDF solution for different mixtures.

5. Acknowledgements

This work is part of the European project KEROGREEN, which has received funding from the European Union's Horizon 2020 Research and Innovation Programme under Grant Agreement 763909. This work is also part of the Shell-NWO/FOM initiative 'Computational sciences for energy research' of Shell and Chemical Sciences, Earth and Life Sciences, Physical Sciences, FOM and STW. This work was also carried out under TTW open technology project (grant nr. 15325) in collaboration with Gasunie, Stedin, DNVGL and Ampleon.

6. References

- [1] A. Goede and M. C. M. van de Sanden, *Europhys. News* **47** (2016), 22–26
- [2] P. Diomedea *et al.*, *J. Phys. Chem. C* **121** (2017), 19568-19576
- [3] P. Diomedea *et al.*, *J. Phys. Chem. A* **122** (2018), 7918-7923
- [4] V. D. Rusanov *et al.*, *Sov. Phys. Usp.* **24** (1981), 447-474
- [5] T. Kozák and A. Bogaerts, *Plasma Sources Sci. Technol.* **23** (2014), 045004
- [6] G. J. M. Hagelaar and L. C. Pitchford, *Plasma Sources Sci. Technol.* **14** (2005), 722-733
- [7] Phelps database, www.lxcat.net, retrieved on October 5, 2018
- [8] E. Hairer and G. Wanner, *Solving Ordinary Differential Equations II*, Springer-Verlag (1996)